*Work supported in part by the U.S. Air Force Office of Scientific Research, under Contract No. AF-AFOSR-1273-67.

†Present address: Dept. of Physics and Astronomy, U. of Toledo, Toledo, Ohio 43606.

[1]R. W. Hill and B. Schneidmesser, Z. Physik Chem. Neue Folge, Bd. 16, 257 S (1958).

[2]C. Ebner and C. C. Sung, preceding paper, Phys. Rev. B 2, 2115 (1970).

[3]W. Hardy and J. R. Gaines, Phys. Rev. Letters 17, 1278 (1966).

[4]NBS Monograph No. 10 (US GPO, Washington, D. C., 1960).

[5]H. Fritzsche, Phys. Rev. 99, 406 (1955).

[6]P. Lindenfeld, Rev. Sci. Instr. 32, 9 (1961).

[7]R. W. Hill and O. V. Lounasmaa, Phil. Mag. 4, 785 (1959).

[8]J. Jarvis, D. Ramm, and H. Meyer, Phys. Rev. Letters 18, 119 (1967).

[9]A. B. Harris, L. I. Amstutz, H. Meyer, and S. M. Meyers, Phys. Rev. 175, 603 (1968).

[10]L. I. Amstutz, J. R. Thompson, and H. Meyer, Phys. Rev. Letters 21, 1175 (1968).

PHYSICAL REVIEW B VOLUME 2, NUMBER 6 15 SEPTEMBER 1970

Extreme-Ultraviolet Spectra of Ionic Crystals*

Frederick C. Brown, Christian Gähwiller, Hiizu Fujita,†
A. Barry Kunz, William Scheifley,‡ and Nicholas Carrera‡
Department of Physics and Materials Research Laboratory University of Illinois, Urbana, Illinois 61801

(Received 1 April 1970)

The absorption spectra of several ionic crystals were obtained by the use of synchrotron radiation with photon energies in the range 50–250 eV. This range includes thresholds for excitation of both p and d core states. Arguments are given that peaks in the observed spectra are generally due to maxima in the final density of states, rather than exciton phenomena. The chlorine $L_{II,III}$ spectra of NaCl, KCl, RbCl, and even AgCl are very much alike, which can be understood in terms of similar conduction-band structure for these materials. It is suggested that double excitations are not as important as collective effects. The $3d \rightarrow p$ spectra of the Br^- Kr-Rb^+ sequence, as well as the $4d \rightarrow p$ spectra of the I^--Xe-Cs^+ sequence, can be understood by taking into account the spin-orbit splitting of the initial states and the final-state band structure. Very prominent d-to-f resonances were found for compounds containing iodine and cesium. In CsCl and CsBr, structure near 160 eV due to excitation of the cesium N_{III} level shows an unusual antiresonance behavior.

I. INTRODUCTION

Our present knowledge of the optical constants of solids for photon energies in the range 20–200 eV is relatively incomplete. Until recently very few continuum light sources were available for high-resolution spectroscopy in the region of grazing incidence optics, say from 50 to 500 Å. Also it has been generally thought that well-defined or characteristic structure is absent in this high-energy region due to the exhaustion of oscillator strength as well as severe lifetime broadening. Actually, a great deal of structure does exist, and our knowledge of the spectral detail is rapidly being improved through the use of synchrotron radiation. Especially strong efforts are under way at the German electron synchrotron (DESY) in Hamburg and at the Tokyo synchrotron by the INSSOR (Institute for Nuclear Studies – Synchrotron Orbital Radiation) group. In the present paper we present results obtained on a variety of alkali halides at the 250-MeV electron storage ring[1] of the University of Wisconsin Physical Science Laboratory in Stoughton, Wisc.

The spectra presented below are the result of largely exploratory observations carried out on specific sequences of elements in ionic crystals. In general, we would like to know how better to relate optical response and band structure. It is well known that density-of-states and matrix elements are important in optical transitions. This leads us to ask the question: Is it possible to confirm the essential features of recent band calculations on ionic crystals[2–6] by exciting electrons from narrow bands of core states of various symmetry – for example, from s, p, or d levels? On the other hand, what new processes perhaps of a collective nature have to be introduced in order to explain the high-energy optical properties of a solid? How is the situation different in a gas compared to a solid? Are antiresonances due to configuration interactions observable in solid-state spectra as well as for autoinizing transitions of gases?[7] Are excitons actually produced for energies which overlie the continuum, and if so, how important are multiple exciton processes?[8,9]

After a brief description of the experimental

methods in Sec. II the results are presented in Secs. III, IV, and V. Excitation from the chlorine $2p^6$ shell in NaCl, KCl, RbCl, and AgCl is discussed and compared with the band results in Sec. III. Results for the isoelectronic sequence Br^--Kr-Rb^+ are given in Sec. IV, where the materials KBr and RbCl are compared. New features of the spectra can be ascribed to transitions from the $3d^{10}$ shell, mainly to p-like conduction bands. The $4d^{10}$ spectra for the I^--Xe-Cs^+ sequence are discussed in Sec. V for KI, CsCl, and CsI. Strong resonances possibly due to delayed d-to-f absorption as in atoms are found for these crystals. Finally, the implications of these results are discussed in Sec. VI.

II. EXPERIMENTAL METHODS

As mentioned above the 250-MeV electron storage ring at Stoughton, Wisc. was used as a light source for the present high-resolution measurements. By the use of a storage ring instead of a more conventional synchrotron, it is possible to build up and maintain quite a high current of circulating electrons which have lifetimes many minutes or even hours. There are also certain advantages due to the fact that the electrons are highly monoenergetic and the beam is of small stable cross section. Furthermore, an electron energy of 250 MeV is quite suitable for spectroscopic work out to 50 Å in the soft x-ray region. These were pointed out some years ago in a report to the Solid State Panel of the National Research Council.[10] Since that time a number of different groups have been using the storage ring at Stoughton as a light source.

The properties of synchrotron radiation have become well known since the paper of Schwinger[11] and the early experimental tests.[12,13] For example, several accounts of spectroscopic applications have been given.[14–16] These results show that the radiation from each relativistic electron is confined to a narrow cone about the direction of electron motion, and also that the spectral distribution of the radiation is strongly peaked toward a cutoff in the vacuum ultraviolet which depends upon particle energy. The radiation emitted in the plane of the orbit is polarized with electric vector in the orbital plane. Synchrotron light is incoherent so that the radiated intensity just increases with the number of electrons in orbit.

Figure 1 shows an outline of the experimental arrangement used for the present measurements of the transmission of thin films. Synchrotron radiation emitted from a small segment of the electron orbit passes through a pipe tangent to the stainless steel chamber of the storage ring to the common vacuum of an ion pumped separation

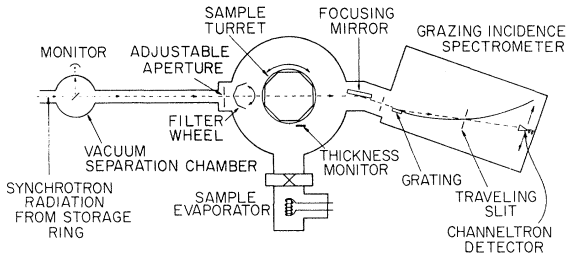

FIG. 1. Apparatus for evaporating and measuring the transmission of thin films in the extreme ultraviolet. Cold baffels surrounding the sample turret are not shown. The entire system was evacuated by means of ion pumps and a turbomolecular pump.

chamber. A small part of the visible radiation in the beam is diverted to a monitor phototube. The main part of the beam passes on through filters into the main chamber where the samples are mounted on the turret (behind cold baffles) of a rotating cryostat. The various alkali halide thin films were evaported *in situ* onto thin Formvar, carbon, or gold substrates whose transmission had been previously measured as a function of wavelength in the extreme ultraviolet. A 5-Mc quartz-crystal thickness monitor calibrated by the Tolansky method enabled the thickness of the deposited layers to be estimated. The various samples with thicknesses ranging from 100 to 3000 Å could be rotated into the ultraviolet beam following evaporation.

After passing through the samples the extreme ultraviolet radiation was focused by a grazing incidence gold mirror onto the 10-μ entrance slit of a 2-m [17] spectrometer with photoelectric recording and a 576-line-per-mm grating (blaze angle 1.6°) used at an angle of 86° to the normal. Photon counting was employed in order to permit the use of small slit widths in the spectrometer and a wide range of beam intensities. The detector was a Bendix extended-cone Channeltron multiplier. A data accumulation system permitted the recording of three channels of information: (i) the signal counting rate (proportional to transmitted uv intensity), (ii) the visible light monitor (proportional to the incident uv intensity), and (iii) the wavelength drum position. This information in digital form was recorded sequentially on a teletype paper-tape punch. Data processing was then completed at the digital computer laboratory of the University of Illinois. A gas cell with very thin polypropylene windows could be inserted in the beam so that the spectrometer could be calibrated against known rare gas lines.

When interference effects are neglected, the transmission of a thin film of thickness d, absorp-

tion coefficient α, and reflectivity R can be written as

$$\frac{I}{I_0} = \frac{(1-R)^2 e^{-\alpha d}}{1-R^2 e^{-2\alpha d}} \ . \tag{1}$$

In the extreme ultraviolet the reflectivity at normal incidence is very small, $R \ll 1$. After approximation only the exponential factor in the numerator of Eq. (1) remains and the absorption coefficient α in cm^{-1} can be determined from the optical density $D = \log_{10}(I_0/I)$ and sample thickness according to the following relation:

$$\alpha d = 2.303 D. \tag{2}$$

In those cases where a reliable estimate of thickness is not available one merely plots the optical density. Of course, the absorption coefficient α and extinction coefficient κ are closely related by the expression

$$\kappa = \alpha\lambda/4\pi \ . \tag{3}$$

It should also be borne in mind that the imaginary part of the dielectric response function $\epsilon_2 = 2n\kappa \simeq \alpha\lambda/2\pi$, since the index of refraction n is very close to 1.000 in the extreme ultraviolet.

When interpreting spectra due to direct transitions between initial bands n and final bands s it is useful as a first approximation to take the square of the matrix elements as a constant $|\overline{M_{ns}}|^2$. In this case the expression for ϵ_2[18] reduces to

$$\epsilon_2(\omega) = \frac{4\pi^2 e^2}{3m^2\omega^2} \, |\overline{M_{ns}}|^2 \sum_{n,s} J_{n,s}(\omega), \tag{4}$$

where $J_{n,s}(\omega)$ is a joint density of states for the bands n and s. Thus $J_{n,s}(\omega)\Delta\omega$ is equal to the number of pairs of states in bands n and s for photon energy $E_s(\vec{k}) - E_n(\vec{k})$ lying within a range $\hbar\Delta\omega$ about $\hbar\omega$. The joint density of states together with the $1/\omega^2$ factor in Eq. (4) are therefore the important quantities for determining the optical spectrum within the framework of these simplifying approximations. Singularities or critical points in $J_{n,s}(\omega)$ (actually, singularities in the final density of states for narrow core initial bands) should then determine the important spectral features.

For some purposes it is instructive to compute and plot the effective number of electrons per atom N_{eff} which contribute to the absorption within a range up to photon energy E_1. The following useful expression can be derived from sum rules and a dispersion relation between ϵ_1 and ϵ_2:

$$N_{\text{eff}}(E_1) = (2m V_0/e^2\hbar^2)\int_0^{E_1} E\,\epsilon_2(E)\,dE, \tag{5}$$

where $E = \hbar\omega$ and the atomic volume $V_0 = A/L\rho$, where A is the atomic weight, L is Avogadro's number, and ρ is the density. When applied to the absorption above a threshold Eq. (5) can be compared with the number of electrons in a given inner shell.

III. 2*p* SHELL OF CHLORINE

A list of energies for the various electron shells of the monovalent elements is given in Table I. Usually such a table is constructed[19] from a combination of electron emission and x-ray absorption or emission data. The energies are then referred to the Fermi level for the element in a condensed state (metal or sometimes ionic crystal). Rather than following this usual procedure Table I was constructed whenever possible so as to refer to the lowest unoccupied band, i.e., the bottom of the conduction band, for ionic crystals. Because of small chemical shifts different compounds are listed separately. In the case of NaCl, KCl, KBr, and KI we have used the values of Norberg *et al.*,[20] which are believed to be accurate to ±0.5 eV or better. In these high-energy photoemission experiments (ESCA) the electron distributions for the various core levels and also the valence bands were directly observed. After correcting for instrument resolution the observed level positions were referred to the valence-band maximum and finally to the conduction-band minimum by adding the known band gaps determined from luminescence excitation spectra by Timusk and Martienssen.[21] In other cases optical threshold were included in Table I when known. For each elements energies were taken from Bearden and Burr.[19] Thus it is possible for some cases when no data are available to take these values and add half the band gap so as to refer to the conduction band. A list of band-gap energies for the alkali, silver, and thallous halides has been compiled (see Table II) using luminescence excitation, two-quantum, and ϵ_2 optical data.

Table I indicates that photoexcitation from the $2p^6$ or $L_{\text{II, III}}$ shell of Cl^- should occur at about 202–204 eV. The observed optical density in this region of photon energy is plotted for NaCl and RbCl in Fig. 2. An $L_{\text{II, III}}$ spectrum for KCl is shown in Fig. 3 (dotted curve), where it is compared with AgCl (solid curve). The alkali chloride results shown here are quite similar to other work[22–24] some of which has been quite recently obtained with the use of synchrotron radiation. Notice that prominent lines or bands are observed with the first line at 201.6 eV in NaCl. At room temperature the peak of this line is chemically shifted to 201.1 eV in KCl and to 201.0 eV in RbCl. Upon cooling the films to 77 °K the spectra shift more or less uniformly about 0.2 eV to higher energies. The lines become

TABLE I. Threshold absorption energies for energy levels of alkali halides and rare gases (in eV).

Z	Element	1s(K)	2s(L_1)	2p($L_{2,3}$)		
2	He	24.58678[a]				
3	Li	54.5[b]				
	LiF	60.2[c]				
	LiCl	59.4[c]				
	LiBr	58.7[d]				
	LiI	58.6[d]				
9	F	685.4[a]	31.[a]	8.6[a]		
10	Ne	866.9[a]	45.4[e]	18.3[a]		
11	Na	1072.1[a]	63.3[a]	30.65[b]		
	NaF			32.0[f]		
	NaCl	1079.6[g]	66.4[g]	33.5[g]		
	NaBr			32.2[f]		
	NaI			32.2[f]		
		2s(L_1)	2p($L_{2,3}$)	3s(M_1)	3p($M_{2,3}$)	
17	Cl	270.2[a]	200.0[a]	17.5[a]	6.8[a]	
	LiCl		201.2[c]			
	NaCl	276.4[g]	202.3[g]	19.3[g]	8.5[g]	
	KCl	279.[g]	202.[g]	19.2[g]	8.4[g]	
	RbCl		199.2[c]			
	CsCl		200.3[c]			
18	Ar	320[a]	244.1[h]	26.5[i]	12.4[a]	
19	K	377.1[a]	293.6[a]	33.9[a]	17.8[a]	
	KCl	379.[g]	297.[g]	37.0[g]	20.5[g]	
	KBr	379.[g]	299.[g]	39.7[g]	20.6[g]	
	KI	379.[g]	296.[g]	36.7[g]	20.1[g]	
		3s(M_1)	3p($M_{2,3}$)	3d($M_{4,5}$)	4s(N_1)	4p($N_{2,3}$)
35	Br	256.5[a]	181.5[a]	69.0[a]	27.3[a]	4.6[a]
	KBr	259.[g]	184.[g]	71.4[g]	31.2[g]	7.7[g]
36	Kr		213.8[a]	90.9[c]	24.0[a]	10.6[a]
37	Rb	322.1[a]	238.5[a]	110.3[a]	29.3[a]	14.0[a]
	RbCl			112.2[c]		15.5[j]
	RbBr					15.7[j]
	RbI					15.6[j]
47	Ag	717.5[a]	571.4[a]	366.7[a]	95.2[a]	55.9[a]
	AgCl					43[c]
	AgBr					43[c]
		4s(N_1)	4p($N_{2,3}$)	4d($N_{4,5}$)	5s(O_1)	5p($O_{2,3}$)
53	I	186.4[a]	122.7[a]	49.6[a]	13.6[a]	3.3[a]
	NaI			52.4[c]		
	KI	189.[g]	126.[g]	51.7[g]	16.0[g]	6.3[g]
	CsI			52.5[c]		
54	Xe		141.3[k]	64.8[k]		
55	Cs	230.8[a]	161.6[a]	76.5[a]	22.7[a]	11.4[a]
	CsCl		160.8[c]	80.0[c]		12.9[l]
	CsBr		160.8[c]			12.8[l]
	CsI		159[c]			12.5[l]

[a]J. A. Bearden and A. F. Burr, Rev. Mod. Phys. 39, 128 (1967). For solids energies are given relative to the Fermi level.
[b]C. Kunz, R. Haensel, C. Keitel, P. Schreiber, and B. Sonntag, Symposium on Electronic Density of States, Washington, D. C., 1969 (unpublished).
[c]Present work.
[d]R. Haensel, C. Kunz, and B. Sonntag, Phys. Rev. Letters 20, 262 (1968).
[e]K. Codling, R. P. Madden, and D. L. Ederer, Phys. Rev. 155, 26 (1967).
[f]R. Haensel, C. Kunz, T. Sasaki, and B. Sonntag, Phys. Rev. Letters 20, 1436 (1968).
[g]See Ref. 20, p. 72.
[h]M. Nakamura *et al.*, Phys. Rev. Letters 21, 303 (1968).
[i]R. P. Madden, D. L. Ederer, and K. Codling, Phys. Rev. 177, 136 (1969).
[j]T. Sagawa *et al.* (unpublished).
[k]R. Haensel, G. Keitel, and P. Schreiber, Phys. Rev. Letters 22, 398 (1969).
[l]H. Saito, S. Saito, R. Onaka, and B. Ikeo, J. Phys. Soc. Japan 24, 1095 (1968).

TABLE II. Band-gap energies of the alkali, silver, and thallous halides (energies are in eV, measured at low temperature, except where noted).

	Li	Na	K	Rb	Cs	Ag	Tl
F	13.6[a]	11.5[a]	10.8[b]	10.3[b]	9.8[b]	...	...
Cl	9.4[c]	8.75[d]	8.7[e]	8.50[f]	8.3[b]	5.1[g]	3.41[h]
		8.0 RT[f]	8.1RT[f]			4.9 RT[g]	
Br	7.6[c]	7.1[i]	7.4[i]	7.2[i]	7.3[b]	4.3[g]	3.01[h]
			7.3 RT[f]			4.0 RT[g]	
I	6.1[c]	5.9[c]	6.34[j]	6.3[i]	6.1[j]	2.92[k]	2.87[f]
			5.8 RT[f]			2.9 RT[k]	
			6.06 RT[j]				

[a]D. M. Roessler and W. C. Walker, J. Phys. Chem. Solids 28, 1507 (1967).
[b]K. Teegarden and G. Baldini, Phys. Rev. 155, 896 (1967).
[c]G. Baldini and B. Bosacchi (unpublished).
[d]T. Miyata and T. Tomiki, J. Phys. Soc. Japan 24, 1286 (1968).
[e]T. Tomiki, J. Phys. Soc. Japan 22, 463 (1967).
[f]T. Timusk and W. Martienssen, Phys. Rev. 128, 1656 (1962).
[g]N. J. Carrera, thesis, University of Illinois, 1970 (unpublished).
[h]R. Z. Bachrach, thesis, University of Illinois, 1969 (unpublished).
[i]D. Fröhlich and B. Staginnus, Phys. Rev. Letters 19, 496 (1967).
[j]J. J. Hopfield and J. M. Worlock, Phys. Rev. 137, A1455 (1965).
[k]S. Tutihasi, Phys. Rev. 105, 882 (1957).
[l]R. Z. Bachrach, Solid State Commun. 7, 1023 (1969).

somewhat higher and a little narrower at 77 °K but here the effect of cooling is nowhere near as dramatic as that for the ultraviolet exciton spectrum. The first lines in the $L_{II,III}$ spectrum have a width at half-maximum of about 0.8 eV (and not more than 20% less at low temperature). On the other hand, the ultraviolet first excitons have widths less than 0.1 eV at low temperature.[25–27] There is a real question whether the peaks seen near 201 eV in Figs. 2 and 3 are excitons or not.

The four spectra shown in Figs. 2 and 3 have a striking similarity. A very similar 2*p* spectrum is found for LiCl (not shown). At first glance this is surprising since the ultraviolet or 3*p* spectrum for LiCl, NaCl, KCl, and RbCl are not so similar. Of course, when comparing soft x-ray with the ultraviolet spectra, one must take into account the larger 1.6-eV[28] spin-orbit splitting of the chlorine 2*p* states. This can be done as pointed out by Sagawa[23] by subtracting the L_{II} spectrum shifted by 1.6 eV and weighted 1:2 as expected for the initial states. Peaks and structure very similar to those shown in Figs. 2 and 3 remain.

One possible way to tell if the first peaks near 201 eV are excitons or not might be to compare their energies with the thresholds for band-to-

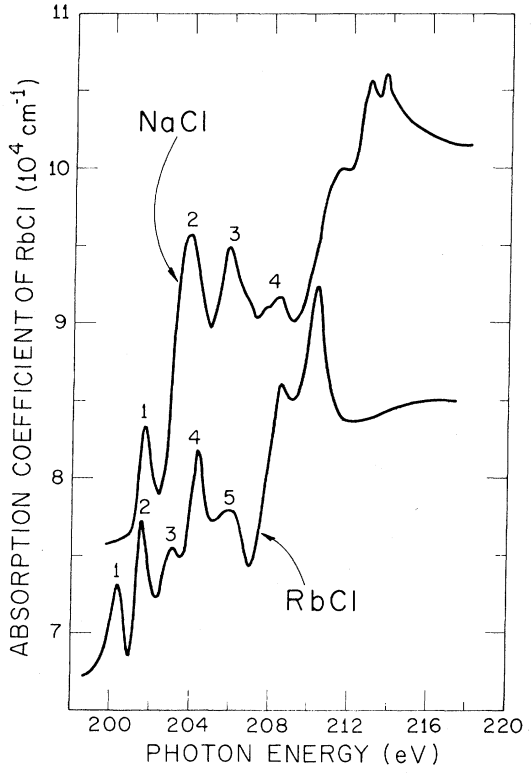

FIG. 2. The $L_{II,III}$ absorption spectra of NaCl and of RbCl at room temperature. The scale on the left applies to RbCl. For NaCl only the optical density in arbitrary units is plotted. The spectral bandwidth is 0.3 eV.

band transitions determined independently.[23] Consider the case of NaCl as an example. One can construct an x-ray energy-level diagram referred to the conduction band by adding half the band gap to the values in Bearden's tables.[19] In this case the L_{III} level of NaCl should be at 204 eV, with a stated uncertainty of about 0.2%. There may be systematic errors here, however, which arise when one combines the various experimental values of binding energy and x-ray emission energy. For these reasons we believe that the more direct measurements of Ref. 20 discussed above should be compared with the optical data. These results are given in Table I and indicate that the L_{III} level of NaCl should be at about 202 eV below the conduction band. This value is uncertain by at least ±0.5 eV, and it also depends critically upon the band-gap energy which was taken as 8 eV. The spectra of Fig. 1 begin quite close to 202 eV; however, enough uncertainty is involved in comparing these two very different measurements that the result is not definitive.

If core excitons predominate near the $L_{II,III}$ edge they should have at least as small binding energies as the ultraviolet excitons (0.4 eV in KI and certainly less than 0.5 eV in most other cases).[29] The effect of ionic as well as electronic polarizability should be felt in both cases since the electron is in similar final states. Moreover, for the x-ray exciton, the hole is highly localized so that central cell corrections to the elementary exciton model are less important. The Wannier or hydrogenlike exciton picture may have to be modified, but in any case when one attempts to estimate the effective dielectric constant it is not the high frequency of excitation which is important but rather the internal motion of electron around the hole. Therefore, we argue that exciton effects are less important than previously thought[23] for the L edge. Binding energies are fairly small compared to linewidths and the oscillator strength for exciton lines is relatively small.[27] Core exciton lines are also very likely broadened by lifetime effects. This point of view has recently been used by Kunz[5,30] in comparing the results of a new, more correct type of band calculation for LiCl with experiment. Having made the point that exciton effects are likely small, let us now attempt an interpretation in terms of existing band structure for the alkali chlorides.

We assume that the optical response is given by Eq. (4) which expresses $\epsilon_2 = 2n\kappa \simeq \alpha\lambda/2\pi$ in terms of density of states. We realize that matrix elements are important but expect that critical points in the conduction-band density of states largely determine the spectrum (taking proper account of selection rules). In Fig. 2 the bands labeled 1–5 have the energies 200.5, 201.5, 203.0, 204.5, and 206 eV, respectively, for RbCl at room temperature. The band structure of NaCl[2] is given in Fig. 4 and of RbCl[4] in Fig. 5. The ordering and relative

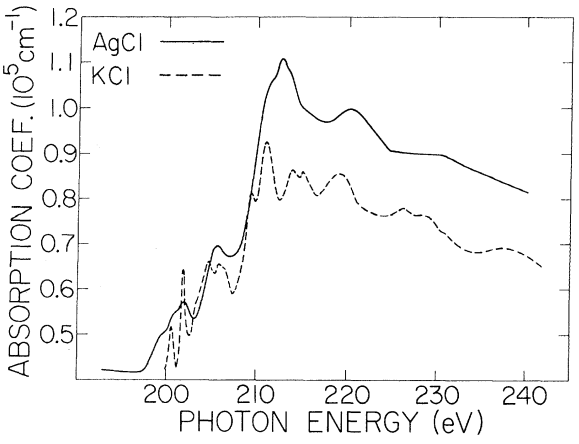

FIG. 3. The absorption coefficient of AgCl and of KCl (arbitrary units) in the chlorine $L_{II,III}$ region at room temperature. The spectral bandwidth is about 0.3 eV.

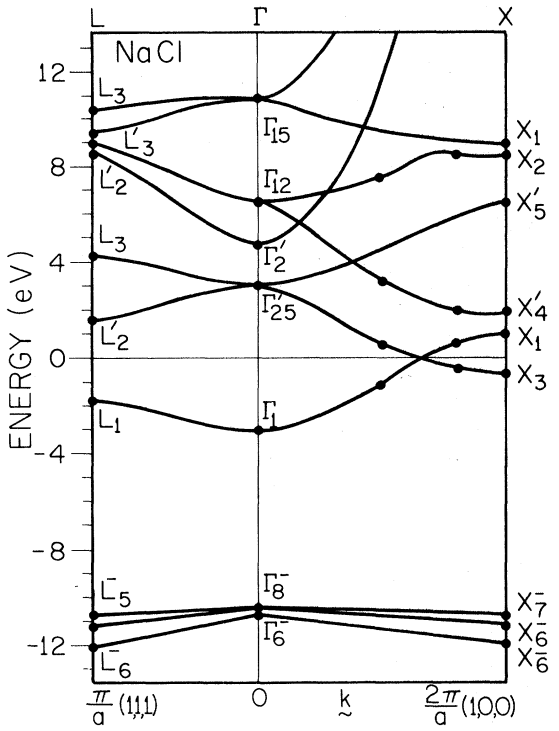

FIG. 4. Band structure of NaCl calculated by the orthogonalized-plane-wave method after Kunz (Ref. 2). Valence bands are shown in the lower part of the figure and the lowest unoccupied point is at Γ_1 in the conduction bands.

position of the conduction-band states for KCl[2] are almost identical to Fig. 5 for RbCl, so we have not bothered to reproduce the figure for KCl. Transitions from the $L_{II,III}$ states to most principal points of the lower conduction bands are allowed except that the wave function in the vicinity of the halogen at L'_2 is p-like, therefore, not allowed. (There are, however, some s and d wave functions on the alkali ion even in this case.) Transitions exactly at X'_4 (p-like) and at Γ'_2 (f-like) are not allowed. However, transitions can occur away from these points due to admixture of wave functions.

Although transitions to the conduction-band minimum at Γ_1 are allowed they should be weak (only a few percent) because there is not a very high density of states in the vicinity of this minimum. This can be seen from the low degeneracy of this s band as well as the calculated density curve of Fong and Cohen[3] for NaCl near threshold. The distinction between M_0, M_1, M_2, and M_3 singularities should be kept in mind. Also, the band diagrams shown are not complete. The [110] direction is not shown and a peak in density of states can arise from *a region* rather than a point in k space. We suggest that peaks 1 in Fig. 2 arise because of transitions from L_{III} mainly to the Δ-Σ-Λ region just above X_3 and approaching L'_2. Away from the region of accidental degeneracy at Δ, the bands tend to flatten, giving rise to appreciable density. Peak 2 is then to be ascribed to Γ'_{25} and X_1 (plus an underlying spin-orbit split component from L_{II}). The weak peak 3 in RbCl may well be due to Γ'_2, and the strong peak 4 is almost certainly due to a high density near Γ_{12} leading out to L'_3. The next singularity peak 5 relates to X_1 and X_2. The second peak associated with Γ'_{25} appears broader and slightly different in NaCl as compared to RbCl or KCl. This may be due to the fact that Γ'_{25} is well above X_1 in NaCl, as can be seen in Fig. 4. It is also true that the fourth peak as well as the Γ_{12}-Λ-L'_3 region is different in NaCl compared to RbCl and KCl. These assignments are tentative but appear reasonable. The great similarity in the $L_{II,III}$ spectra is due to the fact that the conduction bands of the alkali chlorides are all very much alike.

Even the conduction-band structure of AgCl[31,32] and KCl are somewhat similar (except that the order is different at X), which may explain the agreement between AgCl and KCl seen in Fig. 3. Note the greater linewidths for AgCl.

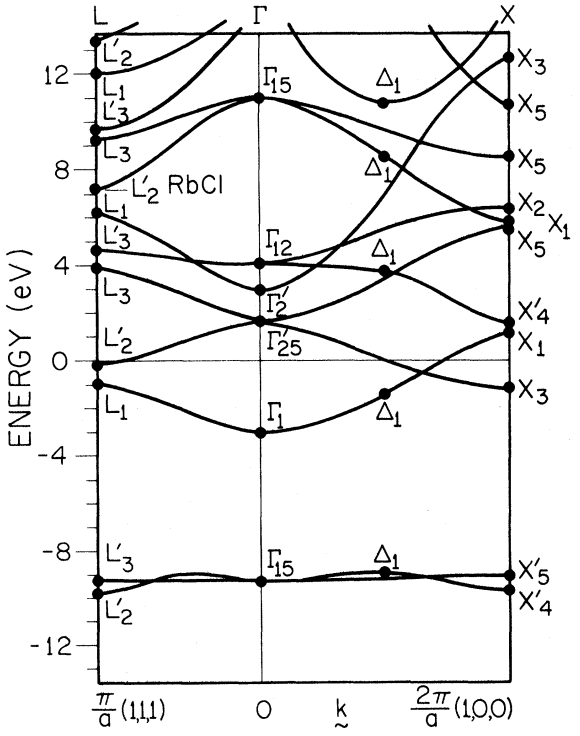

FIG. 5. Band structure of RbCl calculated by the orthogonalized-plane-wave method after Kunz (Ref. 4).

Let us now consider the prominent structure and increasing absorption beginning near 209–211 eV in all cases (Figs. 2 and 3). Close examination suggests that at least the first two components (209 and 212 eV) of this absorption is a replica of lines 1 and 2. Because the shift is about 9 eV, which is approximately the ultraviolet exciton energy (more precisely, the shift is 9, 5 eV in NaCl and 8. 5 eV in RbCl, whereas the room-temperature exciton energies are 7. 73 eV in NaCl and 7. 5 eV in RbCl), it has been suggested[23] that a double exciton process is involved. However, Fig. 3 shows similar structure for AgCl at about 9–10 eV above the first peak. Here this can hardly be the threshold for two excitons since the indirect band gap of AgCl at 300 °K is only 3. 08 eV and even the direct band gap is only 4. 9 eV.[33] In our opinion this additional structure at higher energy cannot be explained by double-exciton or even double-band processes. Such a result is also in agreement with recent theoretical work.[9]

It should be noted that the structure above 10 eV is broad and contains more oscillator strength than at the very edge. The situation is similar for the $L_{II,III}$ edge of light elements such as Al and Si.[34] We suggest that a kind of collective electron effect[35] is involved in which the particle-hole transition is accompanied by a collective excitation of the L shell. In other words when Coulomb interaction between the electron-hole pair and the other possible high-energy excitation pairs is taken into account the unperturbed pair energy is modified or shifted to high energy. The energy shift can be calculated but this does not prove that the collective excitation (plasmon) is well defined. It seems likely however that such is the case. Normally one does not consider that the inner shell electrons are involved in a plasma oscillation. Here, however, the hole in the inner shell is strongly interacting with nearby electrons (even with electrons on neighboring atoms through the long-range Coulomb potential associated with such a defect). It may also be possible that excitations involving a larger number of electrons including the outer shells are possible. One has to look for periodocities especially where well-defined plasmon frequencies are known to exist.[36] Clearly, more theoretical work has to be done in order to verify these ideas.

The excitation of p shells on the alkali ions in ionic crystals gives similar results. This is indeed found to be the case from the careful work by Haensel *et al.*[37] and also of Sagawa and Nakai[38] on the sodium $2p$ shell. The threshold for these transitions occurs in the vicinity of 32 eV as shown in Table I. They will not be discussed further here.

IV. BROMINE KRYPTON RUBIDIUM SEQUENCE - 3*d* ELECTRONS

An interesting isoelectronic sequence is to be found in the bromine ion Br^-, krypton atom Kr, and rubidium ion Rb^+. These all have the krypton core consisting of the argon core plus the following closed shells: $3d^{10}4s^24p^6$. A glance at Table I shows that the bromine $3d$ M_V level in KBr is 71. 4 eV below the lowest conduction band as measured by high-energy electron emission.[20] In krypton gas the corresponding level is around 90 eV and in rubidium 110 eV (see Table I). We have investigated these elements in this region of the spectrum giving special attention to excitation of d-shell electrons to empty conduction bands for solids.

Figure 6 shows the absorption coefficient of KBr from 65 to 200 eV at room temperature. The spectra change only slightly upon cooling to low temperature. Notice the fairly sharp spectral detail extending from 72 to 80 eV followed by a shoulder and then a broad rise to much higher energy. Beginning at 183 eV we see the Br^- L_{III} level (refer to Table I or Ref. 20) followed by the L_{II} level at 190–192 eV. The structure just above 72 eV is shown on an expanded scale in Fig. 7 which is taken from a scan with the KBr film at 77 °K. The broad, almost featureless, rise from 85 to 180 eV may in part be due to excitation of the $3d$ electrons of bromine to f-like final states in the KBr conduction band. There is some analogy between such transitions in the solid and the excitation of the corresponding closed-shell gas atoms.

Figure 8 shows the p excitation states of krypton obtained in our apparatus under the same experimental conditions as the KBr spectra except that a gas cell with polypropylene windows was inserted into the far ultraviolet beam instead of the solid film. The spectrum is very similar to the krypton gas spectrum reported in the literature.[39–41] The energy calibration of our spectro-

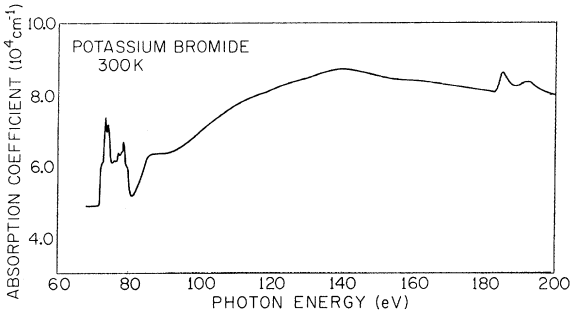

FIG. 6. Absorption coefficient of KBr from 65 to 200 eV. A spectral bandwidth of about 0. 09 Å was employed.

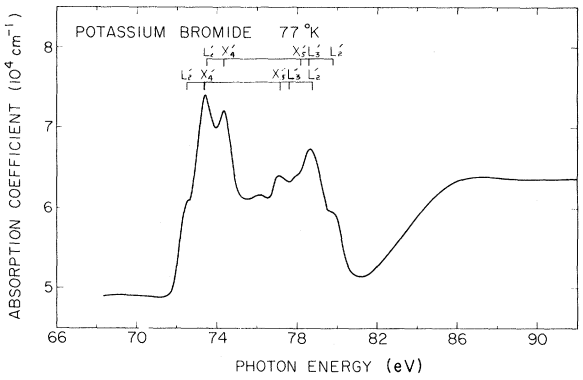

FIG. 7. The d-to-p spectral region for KBr at 77 °K on a greatly expanded scale. The two ladders shown refer to the band diagram of Fig. 9 below and are displaced by the initial-state spin-orbit splitting of 1.0 eV.

meter was checked by comparison with the Kr line positions of Codling and Madden,[39] and from Fig. 8 it can be seen that the energy resolution in this range is about 0.06 eV. Note from the energy scales that these gas lines are about one-tenth as wide as the Br^- bands shown for the solid in Fig. 7. Two series of Kr gas lines are seen separated by the 1.22-eV spin-orbit splitting of the initial states. These series are due to transitions of the type: $\ldots 3d^{10}4s^24p^6$ to $3d^94s^24p^6np$, where the first line in each series corresponds to $n=5$.[39] The $^2D_{5/2}$ series limit occurs at 93.81 eV and the $^2D_{3/2}$ series limit at 95.03 eV.

If we now carry over to the ionic solid these ideas about bound excited states of rare-gas atoms an apparent, although not essential, difficulty arises. The closed-shell Br^- ion occurs in KBr because of the transfer of an electron from the alkali to the halogen (something which is not energetically favored for the isolated molecule). The closed-shell Br^- ion is negative. If a strict *atomic* picture is adhered to, excitation of a d electron leaves a neutral atom without a core potential for hydrogen-like bound excited states. Of course, the way out of this apparent difficulty is to include the surrounding ions of the lattice. A Madelung potential, as well as other contributions, determines the potential at each site. Exciton states of the crystal can also be introduced usually as corrections to the one-electron band picture (they also arise when the one-electron energy-band calculation is carried out correctly including the excited states of the crystal). Haensel and co-workers[41,42] have interpreted the line structure seen at high energy in the solid rare gases as due to forbidden exciton series.

In the case of our KBr spectrum (Fig. 7) the final states are not necessarily exciton states. The initial states are certainly the fairly narrow spin-orbit split $3d$ levels with wave function concentrated mainly on the Br^- ion. The final states are in the normally empty conduction bands and they may have predominantly p-like symmetry. Energy-band calculations for KBr[4] (see Fig. 9) show that the lowest unoccupied states have s-like symmetry and are at the center of the Brillouin zone at Γ_1. It is well established that the characteristic ultraviolet absorption begins with an allowed exciton at 6.9 eV associated with the Γ_{15} (p-like) to Γ_1 (s-like) transition. The $L_{II,III}$ transitions above 183 eV are also of this type but with excitons being less apparent mainly due to lifetime broadening. On the other hand, transitions to Γ_1 from the Br^- $3d$ bands are forbidden, and as before the final density of states are relatively small. In KBr, states with an admixture of p-like wave functions begin about 3 eV higher at the points L_2' and X_4'. In agreement with the spectra of Fig. 7 these p-like band states extend for another 8 eV or so until the upper Γ_{15} point at the center of the Brillouin zone. We do not think that second-class or forbidden excitons with p envelope function (constructed out of the d and Γ_1 states) are important at 72 eV. They would be very weak and followed by much stronger transitions in the vicinity of L_2', X_4', etc., unlike the spectrum of Fig. 7. We are therefore inclined to interpret Fig. 7 in terms of d-to-p-like band transitions with final states beginning a few electron volts above the conduction-band minimum. A reasonable assignment is shown by the two ladders displaced by the Br^- $3d$ spin-orbit splitting of about 1.0 eV.

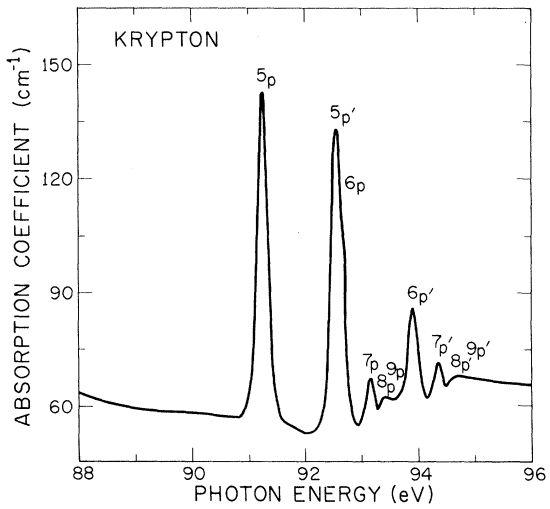

FIG. 8. The krypton gas spectrum in the d-to-p excitation region on a greatly expanded scale. A spectral bandwidth of about 0.06 eV was employed.

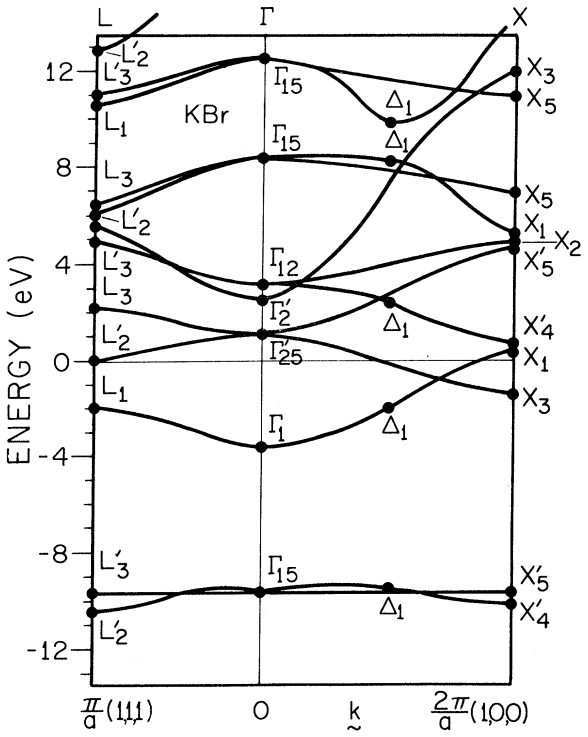

FIG. 9. Band structure of KBr calculated by the orthogonalized-plane-wave method after Kunz (Ref. 4).

Rather than ascribe the peaks to points in the Brillouin zone, we again believe that they belong mainly to maxima in density of states and frequently to a region in k space. For example, the absorption labeled L_2' may begin with density away from the principal direction, near the accidental degeneracy, above X_3 as much as at L_2'.

One expects that d-to-f-like transitions can occur in solids as well as atoms. The lowest f-band state is Γ_2' at 4.0 eV in Fig. 9. Transitions to states in this vicinity may cause the relatively small peak at 76 eV in Fig. 7. Note that this band sweeps rapidly upwards with another crossing point in the [100] direction at about 10 eV. It may be that density in the Brillouin zone away from the principal direction again produces the rise in absorption beginning around 82 eV in Figs. 6 and 7. The long broad maxima extending to much higher energies may then partially be due to delayed d-to-f transitions as discussed by Fano and Cooper.[43] Such an effect is much less important here than in the case of the I^--Xe-Cs^+ resonances discussed in the next section.

This type of analysis is nicely confirmed by the Rb^+ $3d$ spectra shown beginning at 113 eV in the top part of Fig. 10 and on an expanded scale in Fig. 11. The spin-orbit splitting of the rubidium $M_{IV,V}$ levels is 1.5 ± 0.2 eV.[19,28] Figure 11 clearly shows that the various peaks in the d-to-p spectrum occur in pairs separated by precisely the spin-orbit splitting. They also seem to reflect the 6:4 weighting of the $j=\frac{5}{2}, \frac{3}{2}$ initial states. A tentative assignments is made to regions of high density near the points shown where we refer to the band structure of RbCl[4] reproduced in Fig. 5.

V. IODINE XENON CESIUM SEQUENCE - 4d ELECTRONS

The careful electron emission data of Norberg *et al.*[20] on KI indicate that the $4d$ $N_{IV,V}$ levels of iodine lie at 53.3 and 51.7 eV relative to the conduction-band Γ_1 minimum. This is probably one of the more favorable cases for such a measurement since the spin-orbit splitting (1.6 eV from the above numbers) is well resolved, and also the band gap is well known for KI. A $4d$ spin-orbit splitting of 1.6 eV is close to the calculated value.[44]

Figure 12 shows the conduction-band density of states calculated for potassium iodide. For this purpose a pseudopotential interpolation scheme was developed in order to closely approximate the results of the orthogonalized-plane-wave calculation reported in Ref. 44. It was then possible to compute, by means of a large high-speed digital computer, the density of states at 500 nonequivalent points within $\frac{1}{48}$th of the Brillouin zone. The histogram of Fig. 12 is the result. In order to interpret the $4d$ spectrum a $N_{IV,V}$ joint density-of-states curve is constructed. For this purpose, two density-of-states curves were superimposed,

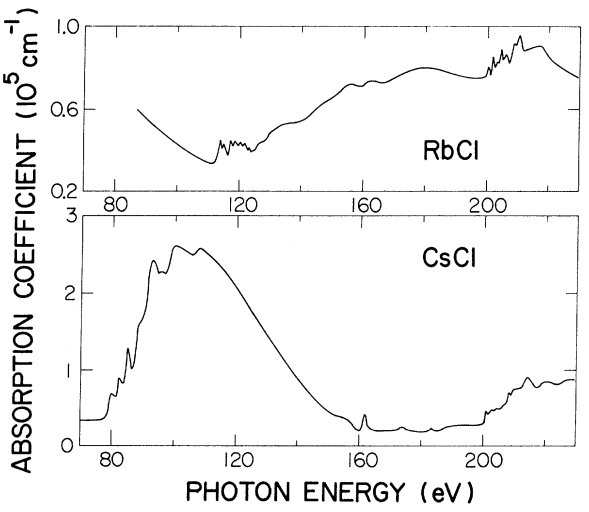

FIG. 10. Absorption spectra of RbCl (upper) and CsCl (lower) from 70 to 230 eV. A great deal of detailed structure above 200 eV was resolved for CsCl but is not shown on this scale.

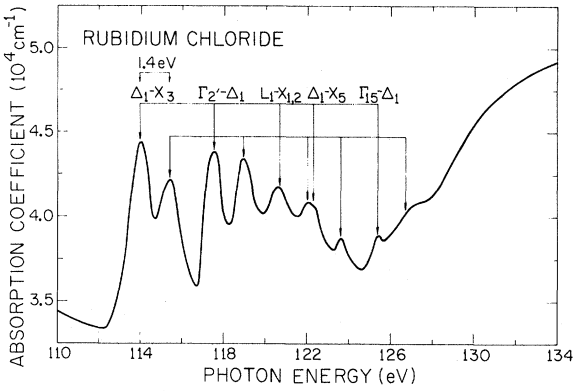

FIG. 11. Absorption spectra of RbCl in the $3d$-to-p region. Notice that the lines occur in pairs. The two ladders shown refer to the band diagram of Fig. 5 and are displaced by the initial-state spin-orbit splitting of 1.4 eV.

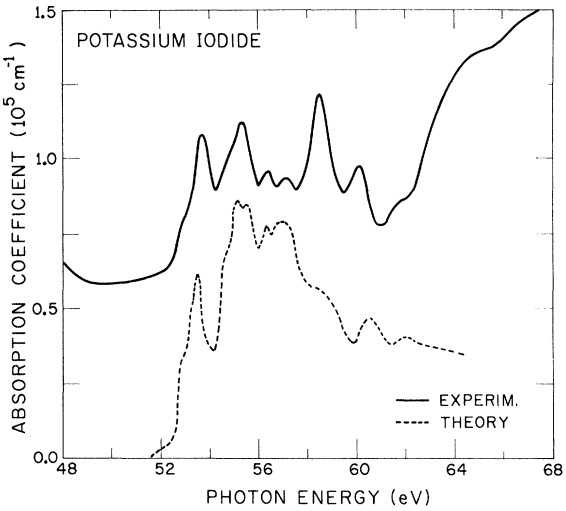

FIG. 13. Observed $4d$ spectrum for KI at 77 °K is shown in the upper part of the figure. A calculated $N_{IV,V}$ joint density of states is shown in the lower part of figure.

weighted in the ratio 6 : 4 according to the $j=\frac{5}{2}$, $\frac{3}{2}$ initial states, and shifted by the 1.6-eV $N_{IV,V}$ spin-orbit splitting. The theoretical curve is then aligned with the absorption threshold, as shown in the lower part of Fig. 13. In the upper part of Fig. 13 we show the observed spectrum which begins about 1 eV above the 51.7-eV N_V level measured by electron emission. A truly remarkable agreement between theory and experiment is seen especially as to the shape of the first prominent band which arises because of state density in the region above X_3 and below the L_2' minimum as before. Note that each peak of the absorption spectrum corresponds to a maximum in the joint density of states. This is a further evidence that exciton effects are not important and that transitions to the s-like Γ_1 minimum are weak and before the edge. The spectrum is in better agreement with the bands calculated in Ref. 4 (orthogonalized plane wave) than by Onodera *et al.*[6,45] (augmented plane wave). Matrix-element effects have not been included and they could very well be the cause of the decrease near the middle of the d spectrum where the suppressed f threshold occurs at Γ_2'. They also account for the rise beyond 64 eV (d-to-f continuum transitions), as explained below.

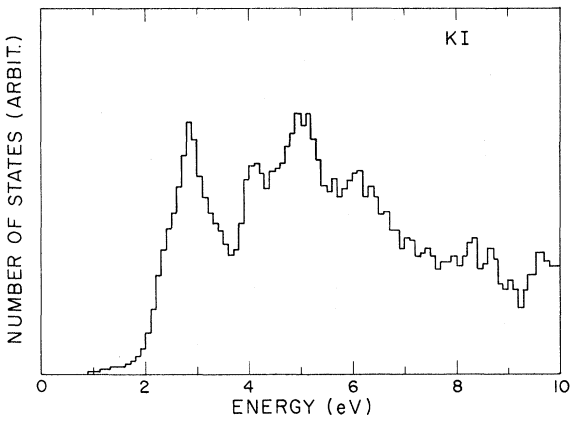

FIG. 12. Calculated conduction-band density of states for potassium iodide from the band structure of Ref. 44.

The photoabsorption spectrum of xenon gas is analogous to the KI d-to-p bands discussed above. In the case of the gas two series of lines separated by about 2 eV are observed between 65 and 70 eV.[39,40,42] These series are ascribed to transitions of the type $\ldots 4d^{10}\,5s^2 5p^6$ to $\ldots 4d^9\,5s^2 5p^6 np$, where the first line in each series corresponds to $n=6$.

The closed-shell ions I^- and Cs^+ have the same electronic structure as atomic xenon, $\ldots 4d^{10}5s^2 \times 5p^6$. Figures 10 and 14 show the absorption spectra of CsCl, KI, and CsI. Note that a strong broad absorption band extending from about 80 to 130 eV occurs in all three cases. In addition, it can be seen that the d-to-p structure near threshold is different in each case. Spectra similar to these and including NaI have been previously published.[46] Comparison of the upper and lower parts of Fig. 10 illustrates how much more important the large resonance is in CsCl than in RbCl. The giant resonance seen in the iodine and cesium compounds is atomic in origin in the sense that a very similar spectrum has been reported by Ederer[47] for xenon gas. It has also been studied more recently for both gaseous and solid xenon by Haensel and co-workers.[42]

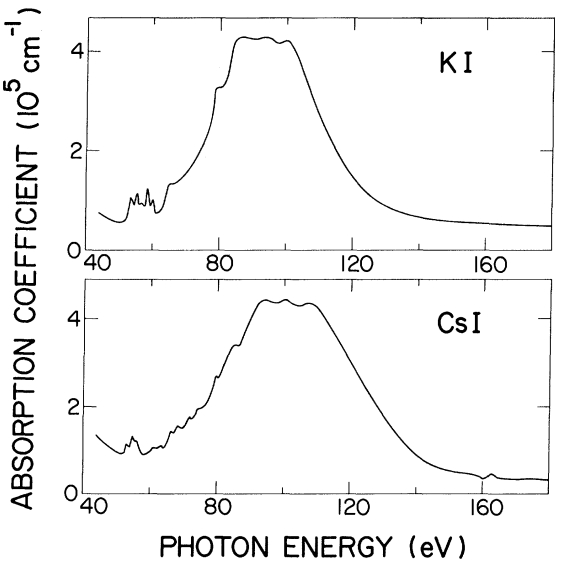

FIG. 14. Absorption spectra of KI and of CsI from 40 to 180 eV showing the d-to-f resonance.

Fano and Cooper[43] have given an explanation which involves d-to-f transitions for the resonances seen in the heavy-rare-gas spectra. Their explanation rests essentially on matrix-element effects. Transitions at the f threshold are somewhat suppressed because the final f-state wave function does not penetrate and overlap appreciably with the d core wave function. Above threshold, where the final-state electron has kinetic energy, the zeros of the wave function move in toward the origin and increasing overlap with the $4d$ core occurs. At still higher energies, the oscillator strength becomes exhausted, and the $1/\omega^2$ term in Eq. (4) is also felt. Such effects are closely associated with the balance between Coulomb potential and the $l(l+1)/r^2$ term in the radial wave equation for the atom. It is interesting that these resonances appear so similar in the gaseous and solid states. They should occur for other nearby elements in the periodic system, for example, compounds containing tellurium and also barium.

It should be pointed out that the strength and to some extent the shape of the d-to-f band is noticeably different in CsI than in the other cases. Also, the position of the cesium resonance in CsCl is displaced about 15 eV to higher energies than the iodine resonance in KI (or in NaI) because of the higher atomic number and different core potential. Actually, unlike the other cases, the resonance in CsI arises from transitions on both the anion and on the cation lattice. This is best seen by evaluating the effective number of electrons N_{eff} by applying Eq. (5). For this purpose the summation was carried out from about 60 to 150 eV after subtracting an extrapolated background. The values of N_{eff} obtained for CsCl, KI, and CsI were 6.2, 11.5, and 16.6, respectively. These numbers are very approximate but they reflect the fact that ten $4d$ electrons on each heavy ion contribute to the resonances.

It should be remarked that definite structure appears superimposed upon the large resonances of Figs. 10 and 14. This structure is reproducible and becomes slightly more pronounced for films cooled to liquid helium temperatures. The step at 80 eV in KI and at about 90 eV for CsCl are located where multiple excitations should occur as in xenon gas. Similar features have also been found in solid xenon.[42]

The high-energy line seen in Fig. 10 for CsCl at about 160 eV is reproduced in Fig. 15 along with similar structure for Xe gas. These are due to the $4p_{3/2}$ states of cesium, the N_{III} level in x-ray notation. At least three lines can be seen in the gas and these most likely correspond to excitation of a $4p$ electron to $6s$, $7s$, and possibly $8s$ excitation states of the atom.[39] The split-off N_{II} level is about 8 eV deeper and is not easily seen in the gas. When the sloping background due to the d-to-f resonance is taken into account an antiresonance is seen in the gas with a minimum on the high-energy side of the first line. On the other hand, for the corresponding transition on the Cs^+ ion in the solid, the antiresonance minimum is on the low-energy side of the line corresponding to positive sign of the parameter q as introduced by Fano.[7] Only one line seems to appear in the case of the solid and this is presumably due to excitation of the cesium $4p$ electron to a maximum of density of states in the conduction band. A very similar line shape is observed at 162 eV in CsBr

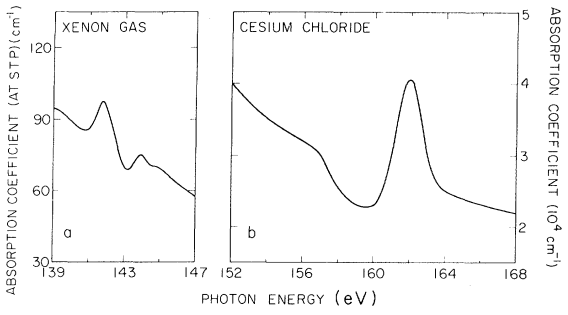

FIG. 15. Absorption coefficient of xenon gas (referred to STP) and of CsCl in the N_{III} region corresponding to excitation of the $4p$ shell. This structure is superimposed on the large resonance seen in Figs. 10 and 14 above (and for the gas in Ref. 42). A very similar line shape was observed for CsBr near 162 eV.

(not shown). The conduction-band structure of the cesium halides is complicated, and it would most likely be very difficult to calculate the line shape including configuration interaction in order to explain the positive q value.

VI. SUMMARY AND CONCLUSIONS

As mentioned in the Introduction a number of specific questions come to mind when one attempts to interpret the high-energy optical response of ionic solids. Some of these have to do with the applicability of existing band calculations, the importance of matrix-element effects and maxima in density of states. New effects such as multiple excitations and collective phenomena are additional possibilities. Just how important core excitons are is worth asking as is the general question concerning the difference in excitation spectrum for a solid as compared to a gas in the extreme ultraviolet. Obviously, we do not have replies to all of these questions at this time, however, some answers are becoming apparent. Moreover, the course of future investigations can perhaps now be better charted.

To begin with, a great deal of structure does exist for ionic solids beyond the LiF cutoff (1050 Å) especially in the vicinity of thresholds corresponding to excitation of the various core levels. Some of the spectral features, such as the large d-to-f resonances in the iodides and cesium halides, are atomic in nature. By this we mean that a very similar band is observed in xenon gas which has the same electronic structure but not the same atomic environment. The resonances in these cases can at least be partially understood in terms of the theory of Fano and Cooper for gas atoms.[43] A superimposed fine structure does exist, however, which may have its origin in collective effects. Other structure at lower energy, such as the lines and shoulders seen near the $3d$-to-p thresholds (70–80 eV) in the alkali bromides and rubidium halides, appears to depend upon the details of the band structure of the solid. The spin-orbit splitting of the initial state must certainly be taken into account. In these cases the lines observed are many times as broad as ultraviolet exciton lines and they do not vary with temperature in the same manner. Although exciton effects may be important we do not think that here they are as important as in the near ultraviolet. This is probably mainly due to small oscillator strength concentrated in the exciton region combined with appreciable lifetime broadening. Very similar remarks can be made about the $4d$-to-p spectra of the alkali iodides and cesium halides as well as the $2p$ edges of the alkali chlorides. Band structure and final density of states determine the spectrum providing that the transition is allowed. When increases source intensity becomes available it would be useful to carry out field modulation experiments in an attempt to confirm some of the symmetry assignments made.

The $4p^6$ levels of cesium in CsCl and CsBr produce edges near 160 eV. These N_{III} levels overlie the strong d-to-f continuum and configuration interaction causes an antiresonance which just preceeds the main absorption in energy.

Finally, whereas the 200-eV $L_{II,III}$ structure of the alkali chlorides as well as silver chloride are alike due to similar conduction-band structure, this same region in CsCl is somewhat more intricate, probably due to a more involved conduction-band detail.

It would clearly be desirable to compute matrix elements as well as density-of-state curves from existing band theory. An even more realistic optical spectrum might then be compared with experiment. Because of the possiblility of collective excitations, which might explain some of the replica structure seen in high-energy spectra, further theoretical work should be carried out. On the experimental side there are certain phenomena to look for, e.g., sidebands and structure which might be seen near edges in high-energy photoluminescence. The yield of such luminescence compared to Auger and other processes should be ascertained. The high-energy optical response of mixed crystals and alloys might be profitably investigated especially near core thresholds. In other words since specific structure is observed for various materials it seems worthwhile to extend the techniques of extreme ultraviolet spectroscopy for analytic purposes. In some cases it may be possible to probe the position of band edges, if not the Fermi level, for varying composition and state of crystallinity. Along somewhat different lines, it appears that high-energy electron emission spectroscopy for the alkali halides, when properly carried out,[20] can be successfully compared with the edges observed in photoabsorption.

ACKNOWLEDGMENTS

The authors are indebted to P. G. Kruger, R. J. Maurer, and M. A. Elango for their interest and suggestions. The continuing support by the University of Illinois staff, especially, F.S. Wise and W. L. Craig, and also by the staff of the University of Wisconsin Physical Science Laboratory, particularly C. H. Pruett, E. M. Rowe, R. Otte, and F. E. Mills, is very much appreciated. One of the authors (FCB) is grateful for an appointment at the Center for Advanced Study, University of Illinois, which made possible his more effective participation in the ultraviolet program.

*Work supported in part by the Advanced Research Projects Agency and the U. S. Army Research Office, Durham, N. C.

†Present address: RCA Laboratories, Inc., Machida City, Tokyo, Japan.

‡Work carried out in partial fulfillment of the Ph. D. requirements, University of Illinois, Urbana, Ill. 61801.

[1]Supported by the U. S. Air Force Office of Scientific Research.

[2]A. B. Kunz, Phys. Rev. 175, 1147 (1968).

[3]C. Y. Fong and M. L. Cohen, Phys. Rev. Letters 21, 22 (1968).

[4]A. B. Kunz, Phys. Status Solidi 29, 115 (1968).

[5]A. B. Kunz, J. Phys. C 3, 1542 (1970).

[6]Y. Onodera, M. Okazaki, and T. Inui, J. Phys. Soc. Japan 21, 2229 (1966).

[7]U. Fano, Phys. Rev. 124, 1866 (1961).

[8]T. Myakawa, J. Phys. Soc. Japan 17, 1898 (1962).

[9]J. C. Hermanson, Phys. Rev. 177, 1234 (1969).

[10]F. C. Brown, P. C. Hartman, P. G. Kruger, B. Lax, R. A. Smith, and G. H. Vineyard, in the National Research Council Solid State Panel Subcommitee Report, 1966 (unpublished).

[11]J. Schwinger, Phys. Rev. 75, 1912 (1949).

[12]F. R. Elder, R. V. Langmuir, and H. C. Pollock, Phys. Rev. 74, 52 (1948).

[13]D. H. Tomboulian and P. L. Hartman, Phys. Rev. 102, 1423 (1956).

[14]K. Codling and R. P. Madden, J. Appl. Phys. 36, 380 (1965).

[15]R. Haensel and C. Kunz, Z. Angew. Phys. 37, 3449 (1966).

[16]R. P. Godwin, in *Springers Tracts in Modern Physics*, edited by G. Höhler (Springer-Verlag, New York 1969), Vol. 51.

[17]A. H. Gabriel, J. R. Swain, and W. Waller, Rev. Sci. Instr. 42, 94 (1965).

[18]H. R. Phillip and H. Ehrenreich, Phys. Rev. 129, 1550 (1963).

[19]J. A. Bearden and A. F. Burr, Rev. Mod. Phys. 39, 125 (1967).

[20]R. Norberg, M. Elango, C. Nordling, and K. Siegbahn (unpublished); see also K. Siegbahn *et al.*, *ESCA Atomic Molecular and Solid State Structure Studied by Means of Electron Spectroscopy* (Almqvist and Wiksells, Uppsala, 1967), p. 72.

[21]T. Timusk and W. Martienssen, Phys. Rev. 128, 1656 (1962).

[22]T. M. Zimkina and A. P. Lukirskii, Fiz. Tverd. Tela 7, 1455 (1965) [Soviet Phys. Solid State 7, 1170 (1965)].

[23]T. Sagawa, Y. Iguchi, M. Sasanuma, T. Nasu, S. Yamaguchi, S. Fujiwara, M. Nakamura, A. Ejiri, T. Masuoka, T. Sasaki, and T. Oshio, J. Phys. Soc. Japan 21, 2587 (1966).

[24]Y. Iguchi *et al.*, Solid State Commun. 6, 575 (1968).

[25]D. M. Roessler and W. C. Walker, Phys. Rev. 166, 599 (1968).

[26]G. Baldini and B. Bossachi, Phys. Rev. 166, 863 (1968); see also Phys. Rev. Letters 23, 846 (1969).

[27]T. Tomiki, J. Phys. Soc. Japan 22, 463 (1967).

[28]H. M. O'Brian and H. W. B. Skinner, Proc. Roy. Soc. (London) A176, 229 (1940); see also F. Herman and S. Skillman, *Atomic Structure Calculations* (Prentice-Hall, Englewood Cliffs, N. J., 1963).

[29]F. C. Brown, in *International Conference on Science and Technology of Nonmetallic Crystals, Delhi, India*, 1969, edited by S. C. Jain (Gordon and Breach, New York, 1970).

[30]A. B. Kunz (unpublished).

[31]P. Scop, Phys. Rev. 139, A934 (1965).

[32]F. Bassani, R. S. Knox, and W. B. Fowler, Phys. Rev. 137, A1217 (1965).

[33]F. C. Brown, J. Phys. Chem. 66, 2368 (1962).

[34]C. Gähwiller and F. C. Brown, Phys. Rev. (to be published).

[35]P. Noziéres and D. Pines, Phys. Rev. 113, 1254 (1959); see also R. A. Ferrell, Rev. Mod. Phys. 28, 308 (1956).

[36]F. C. Brown and C. Gahwiller, Bull. Am. Phys. Soc. 15, 387 (1970); see also T. Miyakawa, J. Phys. Soc. Japan 24, 768 (1968).

[37]R. Haensel, C. Kunz, T. Sasaki, and B. Sonntag, Phys. Rev. Letters 20, 1436 (1968).

[38]T. Sagawa and S. Nakai, J. Phys. Soc. Japan 26, 1427 (1969).

[39]K. Codling and R. P. Madden, Phys. Rev. Letters 12, 106 (1964); see also K. Codling and R. P. Madden Appl. Opt. 4, 1431 (1965).

[40]A. P. Lukuskii, T. M. Zimkina, and I. A. Brytov, Izv. Akad. Nauk SSSR Ser. Fiz. 28, 772 (1964) [Bull. Acad. Sci. USSR, Phys. Ser. 28, 681 (1964)].

[41]R. Haensel, C. Keitel, P. Schreiber, B. Sonntag, and C. Kunz (unpublished).

[42]R. Haensel, C. Keitel, C. Kunz, and P. Schreiber, Phys. Rev. Letters 22, 398 (1969).

[43]U. Fano and J. W. Cooper, Rev. Mod. Phys. 40, 441 (1968).

[44]A. B. Kunz, J. Phys. Chem. Solids 31, 265 (1970).

[45]Y. Onodera, M. Okazaki, and T. Inui, J. Phys. Soc. Japan 21, 816 (1966).

[46]H. Fujita, C. Gähwiller, and F. C. Brown, Phys. Rev. Letters 22, 1369 (1969).

[47]D. L. Ederer, Phys. Rev. Letters 13, 760 (1964).